Cancer Letters 637 (2026) 218120

Contents lists available at ScienceDirect

Cancer Letters

journal homepage: www.elsevier.com/locate/canlet

Original Articles

Caspase-8 is a novel modulator of Homologous Recombination Repair in response to ionizing radiations in glioblastoma

Alessandra Ferri [a,b,2,3], Claudia Contadini [c,3,*], Claudia Di Girolamo [b,d], Claudia Cirotti [a,b], Giulia Fiscon [e,1], Paola Paci [e], Marta Marzullo [f,g], Maria Pia Gentileschi [h], Tatsuro Yamamoto [i], Robert Strauss [i], Donatella Del Bufalo [c], Laura Ciapponi [f], Daniela Barilà [a,b,**]

[a] Department of Biology, University of Rome "Tor Vergata", 00133, Rome, Italy
[b] Laboratory of Cell Signaling, IRCCS-Fondazione Santa Lucia, 00179, Rome, Italy
[c] Preclinical Models and New Therapeutic Agents Unit, IRCCS Regina Elena National Cancer Institute, 00144, Rome, Italy
[d] PhD Program in Cellular and Molecular Biology, Department of Biology, University of Rome "Tor Vergata", 00133, Rome, Italy
[e] Department of Computer, Control and Management Engineering "Antonio Ruberti", Sapienza University of Rome, 00185, Rome, Italy
[f] Department of Biology and Biotechnologies "C. Darwin", Sapienza University of Rome, 00185, Rome, Italy
[g] Institute of Molecular Biology and Pathology (IBPM), CNR, 00185, Rome, Italy
[h] Cellular Networks and Molecular Therapeutic Targets Unit, IRCCS Regina Elena National Cancer Institute, 00144, Rome, Italy
[i] Genome Integrity Unit, Danish Cancer Institute, Strandboulevarden 49, Copenhagen, DK-2100, Denmark

ARTICLE INFO

Keywords:
Glioblastoma
Ionizing radiations
Caspase-8
DNA repair
Homologous recombination
Therapy resistance

ABSTRACT

Caspase-8 is a cysteine protease historically regarded as anti-neoplastic protein, thanks to its role in apoptosis. However, Caspase-8 expression is retained or even enhanced in several tumors, including glioblastoma (GBM), where it plays pro-tumor functions. We previously reported that it is a negative prognostic factor and contributes to resistance against DNA damaging agents, such as ionizing radiations (IR) and Temozolomide, commonly used in standard GBM treatment. We therefore investigated whether Caspase-8 may sustain DNA repair pathways proficiency in GBM. Here we uncover a novel role of Caspase-8 as promoter of the Homologous Recombination Repair (HRR). Importantly, IR promote Caspase-8 transient nuclear translocation and its recruitment to the chromatin. Moreover, Caspase-8 sustains the expression and the recruitment to the chromatin upon IR of RAD51 and CtIP, two key players of the HRR. Consistently, we identify a synthetically lethal interaction between Caspase-8 and PARP inhibition, that may enhance GBM sensitivity to IR. Remarkably, by using Caspase-8−/− murine embryo fibroblasts and a *Drosophila melanogaster* Caspase-8 mutant, we demonstrate that Caspase-8 plays an evolutionary conserved role in DNA repair.

1. Introduction

Glioma is the most frequent brain tumor in adults, accounting for 70 % of all the tumors affecting the central nervous system [1–3]. The most severe form of glioma is glioblastoma (GBM), classified as level IV in the WHO classification. It is extremely deadly, with a dismal prognosis of about one-year survival upon diagnosis [4]. GBM owes its incredible endurance to a multitude of characteristics: its heterogeneity, the abundance of cancer stem cells, its deep infiltrative capacity and over-active DNA repair mechanisms [4,5].

Over the past fifteen years, therapeutic advancements have been limited, with treatment options still largely relying on surgery and ionizing radiation (IR). The addition of Temozolomide (TMZ) offered only modest survival benefits without significantly improving outcomes

* Corresponding author.
** Corresponding author. Department of Biology, University of Rome "Tor Vergata", 00133, Rome, Italy
E-mail addresses: claudia.contadini@ifo.it (C. Contadini), daniela.barila@uniroma2.it (D. Barilà).
[1] Present address: Department for the Promotion of Human Science and Quality of Life, San Raffaele Roma University, Rome, Italy.
[2] Present address: Department of Pathology and Laboratory Medicine, Meyer Cancer Center, Weill Cornell Medical Center, New York, NY, USA.
[3] Equal contribution.

https://doi.org/10.1016/j.canlet.2025.218120
Received 5 June 2025; Received in revised form 24 October 2025; Accepted 7 November 2025
Available online 8 November 2025

[4].

The most severe DNA lesions caused by TMZ and IR are double-strand breaks (DSBs), primarily repaired by Homologous Recombination (HR) and Non-Homologous End Joining (NHEJ) pathways. While NHEJ operates throughout the cell cycle and requires minimal homology to ligate the DNA break ends, HR is restricted to S/G2 phases and ensures high fidelity by using the sister chromatid as a template, thereby reducing the risk of misalignment and illegitimate chromosomal rearrangements [6,7]. In GBM, therapy resistance is partly driven by aberrant activation of these repair pathways, reducing the efficacy of DNA-damaging treatments.

Caspase-8 is a cysteine protease associated with the extrinsic pathway of the apoptotic death program, and it is therefore considered an unfavorable protein for tumour progression. However, the observation that some tumors, including GBM, unexpectedly upregulate the expression of Caspase-8 suggests that, in specific contexts, Caspase-8 may be beneficial for tumour survival [8,9]. Indeed, non-canonical roles of Caspase-8 have been uncovered over the past fifteen years: its activity in controlling cellular motility and encouraging migration [10], its ability to favour tumorigenesis, anoikis resistance [11] and to promote an inflammatory microenvironment and neoangionesis [12,13].

Furthermore, we previously demonstrated that GBM cells silenced for Caspase-8 expression are more sensitive to TMZ and IR, in line with the inverse correlation found between Caspase-8 expression and the overall survival of GBM patients [12,13]. Based on these observations, we investigated whether Caspase-8 expression reduces treatment sensitivity by promoting DNA Damage Repair (DDR).

Here we identified Caspase-8 as a prerequisite for DDR in GBM cells, specifically sustaining the expression and the recruitment to chromatin of HR Repair (HRR) factors. We further provided evidence for a nuclear Caspase-8 localization in GBM cellular models, especially after IR. Remarkably, using murine embryo fibroblasts (MEF) and *Drosophila melanogaster* model, we could show that Caspase-8 sustains DNA repair also in non -tumor and -human contexts and *in vivo,* suggesting a conserved function.

Overall, we identified an interplay between Caspase-8 and HRR in GBM cellular models. Since HR-deficient cancer cells are highly sensitive to PARP inhibition [14–16], we also suggest a synthetic lethality strategy by using PARP inhibitors plus IR to enhance the sensitivity of cancer cells defective for Caspase-8 expression to DNA damage induced by IR.

2. Results

2.1. Caspase-8 expression sustains DNA damage repair in glioblastoma cellular models

Having previously demonstrated that Caspase-8 expression correlates with reduced sensitivity to IR and TMZ in GBM models [12,13], we tested whether Caspase-8 promotes therapy resistance through DDR modulation. To this end, we performed a neutral comet assay to directly measure the amount of fragmented DNA upon treatment with IR. We employed two GBM cell lines (U87-MG and A172), stably expressing either non-targeting shRNA (shCTR) or shRNA against Caspase-8 (shC8) (Fig. 1A,–Fig. S1A). As expected, IR triggers DNA fragmentation independently of Caspase-8 expression, as shown by the length of the comet tails 1 h after IR (Fig. 1B–Fig. S1B). Importantly, 24 h post-IR, shC8 cells showed prolonged detection of fragmented DNA, as indicated by the persistence of the comet tail, differently from the respective shCTR cells (Fig. 1B–Fig. S1B). Moreover, 24 h after IR we observed an increased percentage of cells with micronuclei in shC8 compared to shCTR cells (S1C,D). DNA repair upon IR was also assessed through immunofluorescence analysis of pSer139H2AX (γH2AX), a common marker of DNA damage (Fig. 1C–Fig. S2A), which triggers the recruitment of several DNA repair proteins to the damage site [17]. Interestingly, although shCTR and shC8 cells exhibit comparable γH2AX levels 1 h after IR, shC8 cells retain elevated γH2AX foci 24 h post-IR, in contrast with shCTR cells (Fig. 1C–Fig. S2A). The same result was also obtained using patient-derived GBM stem cells grown as neurospheres (GBM39). These neurospheres were silenced (shC8) or not (shCTR) for Caspase-8 expression (S2B) and their ability to repair DNA damage upon IR was analyzed by immunofluorescence for γH2AX, as above (S2C). Again, Caspase-8 downregulation impairs the repair of damaged DNA (S2C).

Interestingly, phosphorylation levels of pivotal DDR kinases (*i.e,* ATM, ATR and DNA-PK) [17–20] were not reduced in shC8 cells compared to the control ones (S2D), which is consistent with the similar amount of damage observed in both shCTR and shC8 cells 1 h post-IR.

Remarkably, the stable reconstitution of Caspase-8 expression (U87shC8-C8-WT cells) (Fig. 1D), efficiently rescued the DNA damage, as shown in Fig. 1E. Overall, these data support a crucial role for Caspase-8 in the modulation of DDR following the formation of γH2AX foci in response to DNA damage.

2.2. Caspase-8 transiently accumulates in the nucleus and binds chromatin in response to IR

It has been previously reported that Caspase-8 localizes both in the nucleus and cytoplasm in cancer cells [9]. Given the effect of Caspase-8 on DNA repair, we sought to investigate Caspase-8 subcellular localization in our GBM cellular models. Immunofluorescence experiments in U87-MG and A172 cells showed that Caspase-8 localizes both in the nucleus and in the cytoplasm under basal conditions (Fig. 2A). Indeed, pretreatment with Leptomycin, a well-known inhibitor of nuclear export, resulted in a strong accumulation of Caspase-8 in the nucleus, further supporting its ability to shuttle between these two cellular compartments (Fig. 2B). Interestingly, IR induce a transient accumulation of Caspase-8 in the nucleus (Fig. 2C,D) and on the chromatin (Fig. 2E) detectable as early as 30' post-IR. Overall, these data suggest that in basal conditions Caspase-8 shuttles between nucleus and cytosol, while it accumulates into the nucleus and binds chromatin upon IR, further supporting a new role for Caspase-8 in the DDR.

2.3. Caspase-8 regulates RAD51 and CtIP expression and chromatin recruitment after IR

To uncover the significance of Caspase-8 expression in GBM cells, we recently performed transcriptomic [12] and proteomic analyses [21] to study the differential gene and protein expression in U87-MG shC8 or shCTR cells. The transcriptomic analysis highlighted a significant downregulation of genes involved in inflammation, metabolism and interestingly in IR and DSBs response (S3A). Interestingly, Caspase-8 silencing led to a downregulation of genes primarily involved in HRR, but not in NHEJ (Fig. 3A), suggesting that Caspase-8 predominantly affects HRR. Consistently, the proteomic analysis revealed a general reduction of DNA Damage response, DDR and DSBs as well (S3B). Analyzing by EnrichR 44 proteins involved in DNA repair's process, we highlighted a downregulation of factors belonging to HRR (Fig. 3B) and involved in DNA binding (Fig. 3C). To further confirm the role of Caspase-8 in HRR, we evaluated the basal expression and the recruitment to the chromatin upon IR of CtIP (CtBP-interacting protein) and RAD51 recombinase, two key players of the HRR pathway [22,23]. Transcriptomic analyses reveal that shC8 cells display a significant reduction of both CtIP and RAD51 compared to shCTR (Fig. 3D–S3C). Remarkably, the reconstitution of Caspase-8 expression (shC8-C8-WT) rescued CtIP and RAD51 expression levels (Fig. 3E). More interestingly, Caspase-8 silencing impaired their recruitment to the chromatin upon IR (Fig. 3F–Fig. S3D).

Interestingly, Caspase-8 expression positively correlates with HRR signature in glioma (Fig. 3G–Fig. S3E) as well as in several tumors that retain Caspase-8 expression (S3E).

Moreover, the association between CASP8, HRR genes and patient overall survival was evaluated using expression and clinical data from the CGGA cohort (Fig. 3H). For each gene, patients were stratified into

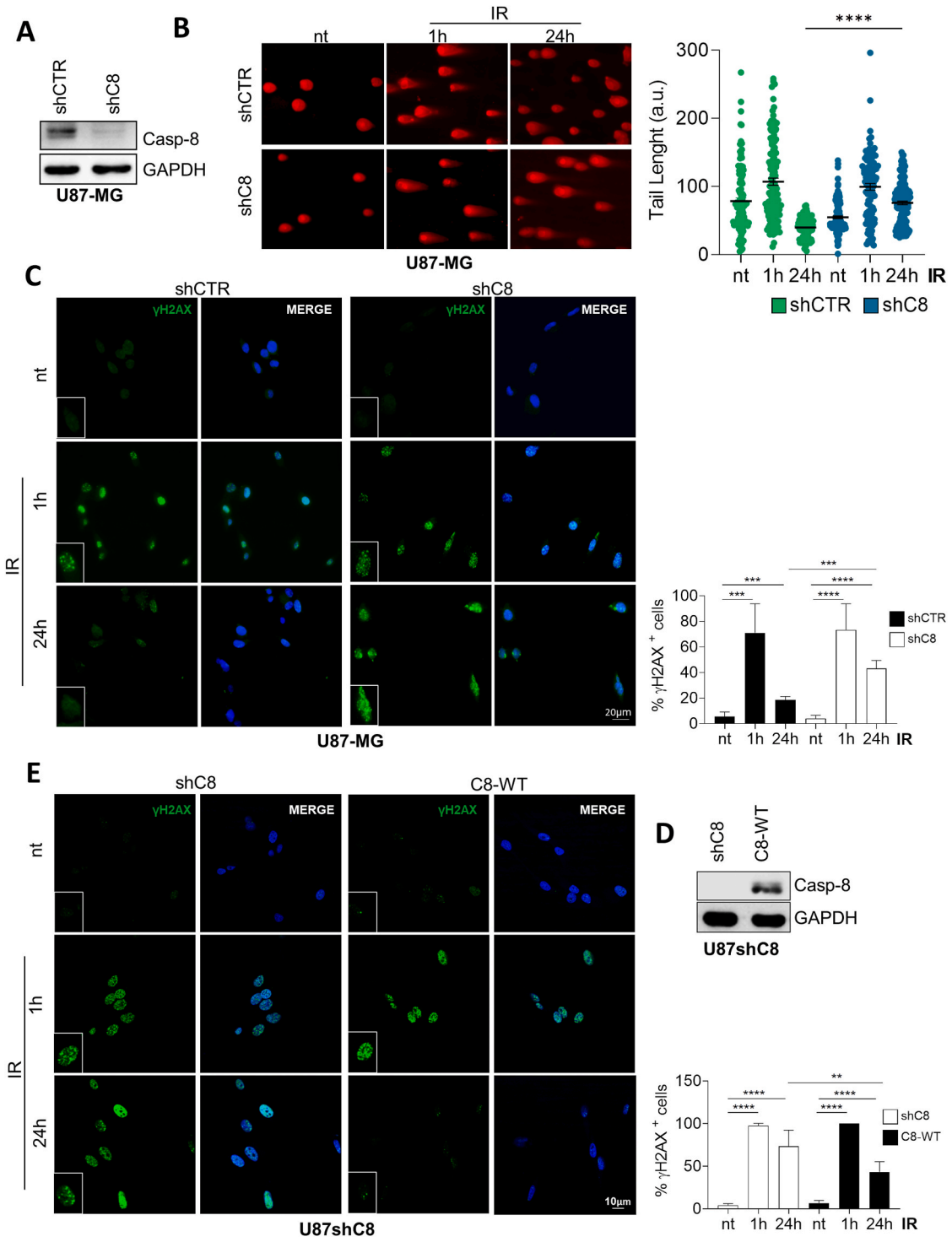

Fig. 1. Caspase-8 expression influences DNA repair capacity of GBM cells. (A) Immunoblotting on total protein extracts from U87-MG stably silenced for Caspase-8 expression (shC8) or not (shCTR). GAPDH was used as loading control. **(B)** Representative images of Neutral Comet Assay showing Comet tails at time 0 (not treated, nt) and 1 h–24 h post IR (5Gy). Graphs representing the median length of the comet. **(C)** Immunofluorescence and relative quantification showing the percentage of U87-MG cells (shCTR *vs* shC8) considered positive for the phosphorylation on Ser139 of the histone variant H2AX (n° γH2AX foci>5) at time 0 (not treated, nt) and 1 h–24 h post IR (5Gy); γH2AX (green), DNA (blue, Hoechst). Scale bar, 20 μm **(D)** Immunoblotting on total protein extracts from U87-MG stably silenced for Caspase-8 expression (shC8) and stably reconstituted for Caspase-8 expression (C8-WT). GAPDH was used as loading control. **(E)** Immunofluorescence and relative quantification showing the percentage of U87shC8 and U87shC8 cells stably reconstituted with C8-WT considered positive for the phosphorylation on Ser139 of the histone variant H2AX (n° γH2AX foci>5) at time 0 (not treated, nt) and 1 h–24 h post IR (5Gy); γH2AX (green), DNA (blue, Hoechst). Scale bar, 10 μm. Statistical analysis was performed by the unpaired Student's t-test (ns = not significant; *P ≤ 0.05; **P ≤ 0.01; ***P ≤ 0.001; ****P ≤ 0.0001). Results represent the mean of three independent experiments ± SD. (For interpretation of the references to color in this figure legend, the reader is referred to the Web version of this article.)

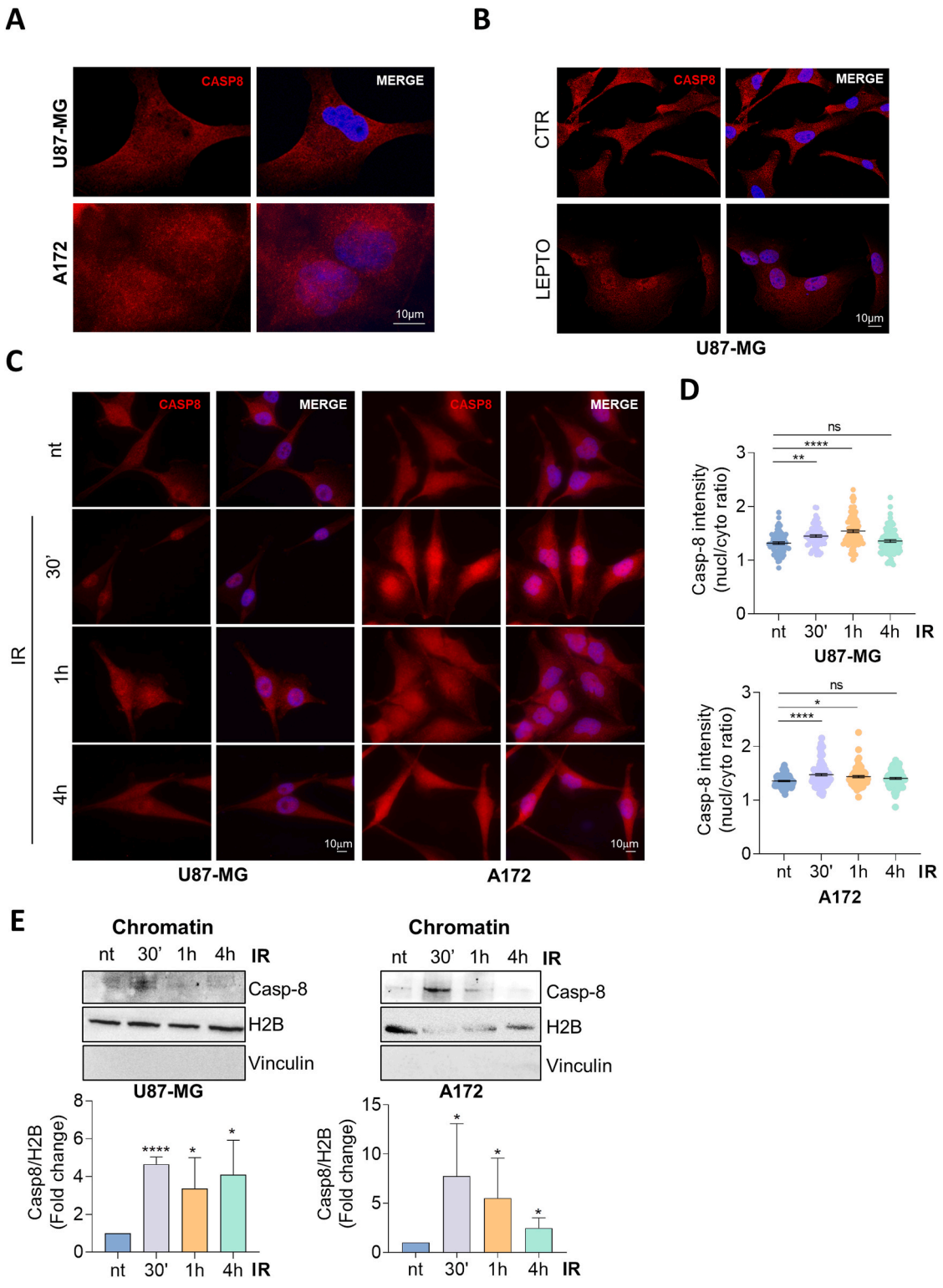

Fig. 2. Caspase-8 shuttles between cytosol and nucleus in basal condition and is recruited on chromatin upon IR. (A) Immunofluorescence showing diffuse staining for Caspase-8 (red) in U87-MG and A172 cells. DNA (Hoechst). **(B)** Immunofluorescence showing an accumulation of nuclear Caspase-8 (red) in U87-MG and A172 cells after treatment with Leptomycin B (20 nM) for 3 h. DNA (blue, Hoechst). Scale bar, 10 μm. **(C–D)** Immunofluorescence and relative analysis of U87-MG and A172 showing Caspase-8 localization at time 0 (not treated, nt) and 30′-1 h–4 h post IR treatment (5Gy). Caspase-8 (red), DNA (blue, Hoechst). Scale bar, 10 μm. **(E)** Immunoblotting and relative densitometric analysis of chromatin insoluble portion derived from U87-MG and A172 cells extracted at time 0 (not treated, nt) and 30′–1 h–4 h post IR (5Gy). H2B was used as chromatin loading control and Vinculin as cytoplasmic contamination control. Statistical analysis was performed by One-way ANOVA statistical test and by the unpaired Student's t-test (ns = not significant; *P ≤ 0.05; **P ≤ 0.01; ***P ≤ 0.001; ****P ≤ 0.0001). Results represent the mean of three independent experiments ± SD. (For interpretation of the references to color in this figure legend, the reader is referred to the Web version of this article.)

two groups based on the median expression value (low and high expression). This analysis unveils that higher expression levels of Caspase-8 and HRR genes are positively correlated with poorer overall patient survival (Fig. 3H), further confirming their relevance to patient outcomes.

2.4. Caspase-8 promotes DNA damage resolution by supporting Homologous Recombination Repair

To further verify whether Caspase-8 impinges on HRR, we performed immunofluorescence analysis of shCTR and shC8 cells upon IR by using Cyclin A as marker of the S/G2 phases, while BRCA1 and 53BP1 as

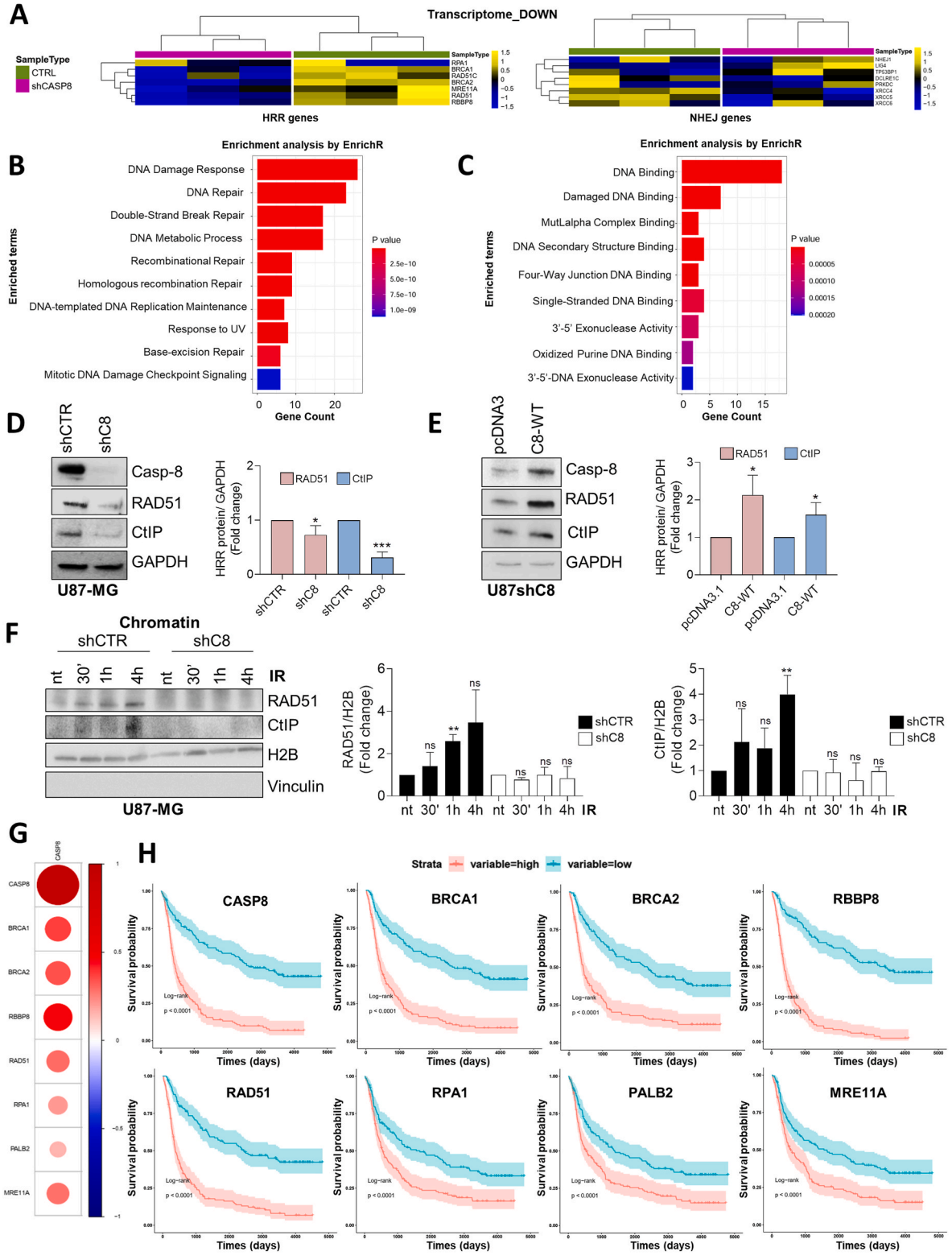

(caption on next page)

Fig. 3. Caspase-8 silencing impairs DNA Damage repair, Homologous Recombination Repair and chromatin recruitment of RAD51 and CtIP upon DNA damage. (A) Heatmaps of expression levels of genes involved in Homologous Recombination Repair (HRR) and Non-homologous end joining (NHEJ) (logarithmic scale) across 6 U87-MG samples grouped by CTRL cells (3 samples, green bars) and shCASP8 samples (3 samples, magenta bars). A z-score normalization was applied and colors represent different expression levels increasing from blue to yellow. Expression profiles are clustered according to samples (columns) of the data matrix by using Euclidean distance as metrics and complete linkage as clustering algorithm. **(B–C)** Barplots showing the enrichment analysis in Gene Ontology Biological Processes (B) and Molecular Function (C) for the 44 genes involved in DNA repair's process. Bars length refers to the number of gens annotated in each category, whereas bars color refers to the p-value of the functional enrichment analysis performed by querying EnrichR tool. **(D)** Immunoblotting and relative densitometric analysis showing CtIP and RAD51 protein level in U87shCTR and U87shC8 cells. GAPDH was used as loading control. **(E)** Immunoblotting and relative densitometric analysis showing CtIP and RAD51 protein level in U87-MG shC8 and shC8 transiently reconstituted for Caspase-8-WT expression. GAPDH was used as loading control. **(F)** Immunoblotting and relative densitometric analysis of chromatin insoluble portion derived from U87shCTR and U87shC8 at time 0 (not treated, nt) and 30′_1 h–4 h post IR treatment (5Gy). H2B was used as chromatin loading control and Vinculin as cytoplasmic contamination control. Results represent the mean of three independent experiments ± SD. Statistical analysis was performed by the unpaired Student's t-test (ns = not significant; *P ≤ 0.05; **P ≤ 0.01; ***P ≤ 0.001; ****P ≤ 0.0001). **(G)** Correlation plot of Caspase-8 gene (CASP8) expression respect to genes involved in HRR. Data refer to expression data from 325 glioma samples extracted from the CGGA (Chinese Glioma Genome Atlas repository). Each dot is colored by Pearson correlation value, with color-scaling from blue (negative values) to red (positive values) and increasing in size with the value of correlation. All correlation values reported are statistically significant, considering an adjusted p-value for multiple comparisons (FDR) < 0.05. **(H)** Kaplan-Meier plots of CASP8 and genes involved into HRR. Patients were stratified into two groups based on the median expression value: low-expression group (cyan curve, patients with expression values lower than the median) and high-expression group (light red curve, patients with expression values higher than or equal to the median). Each reported gene displayed a log-rank p-value ≤0.05. (For interpretation of the references to color in this figure legend, the reader is referred to the Web version of this article.)

markers of HRR [24,25] and NHEJ [26], respectively. As expected, a significant increase of BRCA1 foci number in shCTR Cyclin A^+ cells was detected 1 h post-IR, differently from shC8 which displayed an overall dampened recruitment of BRCA1 on DNA (Fig. 4A,C,Fig. S4A,C). Interestingly, no significant difference in the number of 53BP1 foci post-IR was observed between shCTR and shC8 cells when analyzing only $CyclinA^+$ cells (Fig. 4B,D–Fig. S4B,D), or when considering cells regardless of CyclinA status (Fig. S4E and Fig. S4F).

Furthermore, we assessed the DNA repair pathway choice by using the traffic light reporter system [27] in U87shCTR and shC8 cells. Traffic light reporter assay provides a flow cytometric readout of HRR (GFP) or NHEJ (mCherry) upon DNA damage. In accordance with our previous findings, Caspase-8 silencing consistently reduced HRR capacity, while NHEJ was only affected in a random manner (Fig. 4E–G).

Finally, U87-MG cells depleted or not for Caspase-8 expression were irradiated alongside RAD51 (RAD51i) or DNAPK (DNAPKi) inhibitors, to selectively block HRR and NHEJ, respectively. As expected, both inhibitors slightly increased the sensitivity of shCTR cells to IR (Fig. 4H). Remarkably, U87shC8 cells exhibited greater sensitivity to NHEJ inhibition rather than to HRR inhibition, strongly confirming a role for Caspase-8 in the modulation of HRR (Fig. 4H).

2.5. Caspase-8 activity sustains its nuclear localization, CtIP/RAD51 chromatin recruitment and DNA repair proficiency

To investigate the role of Caspase-8 enzymatic activity in the DDR, we performed experiments on GBM cells using both genetic and pharmacological approaches to inhibit Caspase-8 activity (Fig. 5). In detail, U87shC8 cells were transiently transfected with either Caspase-8-WT or with the catalytic inactive mutant, C8-C360S. Interestingly, we observed that Caspase-8 enzymatic activity is required for its nuclear localization and for DNA repair upon IR (Fig. 5A–C). These results were further confirmed treating U87-MG cells with zIETD-FMK, a specific Caspase-8 inhibitor and inducing DNA damage by IR or Neocarzinostatin (NCS) (Fig. 5D–F–Fig. S5A). Additionally, we observed that Caspase-8 activity is dispensable for the modulation of RAD51/CtIP expression levels (S5B), while it seems to affect RAD51 and CtIP chromatin localization (Fig. 5G).

Overall, these experiments suggest that Caspase-8 enzymatic activity is not required for the expression HRR proteins *per se* but rather it is necessary to allow Caspase-8 nuclear localization and promote the recruitment of HRR factors to chromatin, thereby sustaining DDR.

2.6. Caspase-8 expression sustains DRR in non-transformed in vitro and in vivo models

We further investigated this novel Caspase-8 function in a non-tumoral context, by using murine embryonic fibroblasts (MEF), either *wild-type* (WT) or Caspase-8 *knock-out* (C8−/−).

Analyzing γH2AX via immunoblotting and immunofluorescence, revealed higher γH2AX in C8−/− MEFs 24 h post-IR (Fig. 6A,B), suggesting that the absence of Caspase-8 impairs DDR functionality.

These data suggest that this newly identified non canonical function of Caspase-8 in DDR is also present in a non-tumoral context and is plausibly evolutionary conserved. To verify this, we conducted analogous experiments using *Drosophila melanogaster* Caspase-8 mutant as model system. The *Drosophila* Caspase-8 orthologue, Dredd, has been shown to have a conserved role in apoptosis [28] and to participate in NF-κB-dependent immune functions [29,30]. Specifically, *D44* mutants, which carry mutations in the DED domain, are Caspase-8 defective and display impaired Dredd ability to interact with NF-κB and trigger the immune response [30].

Taking advantage of this mutant, we evaluated the ability of Dredd to mediate DNA repair. *Drosophila* possesses a single histone H2A variant, H2Av, which is thought to fulfill the roles of both mammalian H2A.Z and H2A.X in transcriptional regulation and DDR [31]. To analyze the kinetics of X-ray-induced phosphorylation of H2Av phosphorylated at S137 (γH2Av), $dredd^{\Delta 44}$ and *wild-type* (ctrl) larvae were irradiated with X-rays at 5Gy and γH2Av levels in larval brains were assessed at 0, 10′, 30′, 1 h and 2 h post-IR, by both immunoblotting and immunofluorescence. Immunoblotting revealed that in ctrl γH2Av levels increased at 10′ and 30′ post-IR and decreased at 1- and 2-h post-IR, consistent with canonical DDR kinetics [32]. In contrast, in *dredd* mutants, high levels of γH2Av were retained at 1- and 2-h post-IR, suggesting that the defective Dredd impairs DDR process (Fig. 7A). DNA repair kinetics in larval brains after IR were assessed also through immunofluorescence, quantifying the number of γ-H2Av foci per cell (Fig. 7B,C). Consistent with the immunoblotting data, *wild-type* and *dredd* mutant brains had similar $\gamma H2Av^+$ cells at 10′ and 30' post-IR. However, at 1- and 2-h, *dredd* cells retained more of γH2Av foci than *wild-type*, with the largest difference at 2h post-IR (6.6 vs 8.7 foci per cell).

To assess the role of *Drosophila* Caspase-8 orthologue in apoptosis, we performed TUNEL assays on *wild-type* and *dredd* mutant larval brains. Quantification of TUNEL-positive cells revealed that apoptosis was still detectable in the absence of Dredd and increased after IR, with greater accumulation of apoptotic cells 2 h post-IR compared with ctrl (Fig. S6A), indicating enhanced sensitivity to DNA damage in absence of Dredd.

These data emphasize the crucial role of Caspase-8 in DDR signaling and highlight the *in vivo* conservation of this non-canonical function.

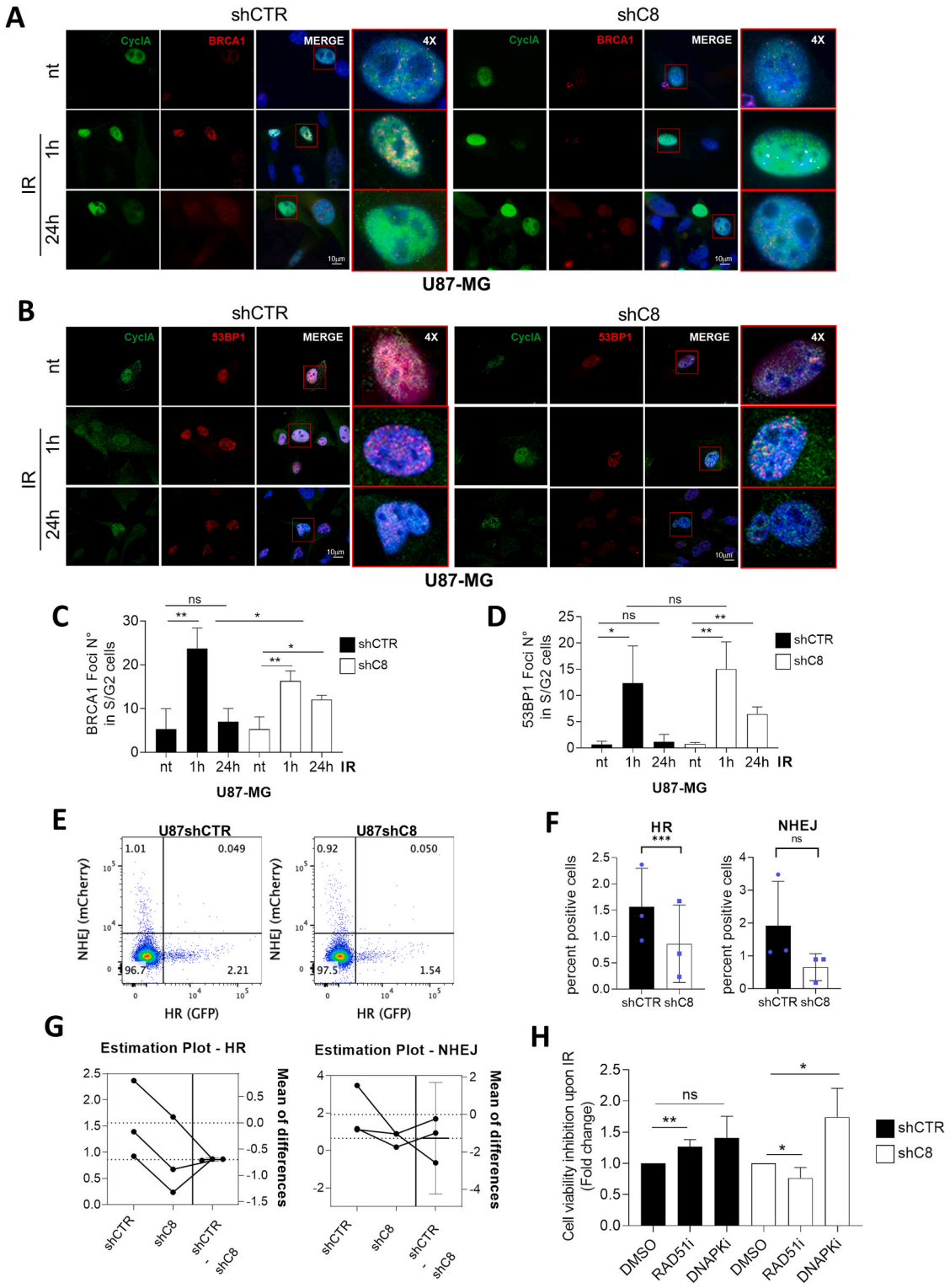

Fig. 4. Caspase-8 exerts its effect on DNA repair influencing proficiency of the Homologous Recombination Repair pathway. (A–B) Immunofluorescence analysis performed on U87-MG shCTR and shC8 cell lines to detect Cyclin A (green) and BRCA1 (**A,** red) or 53BP1 (**B**, red) foci at time 0 (not treated, nt) and 1 h–24 h post IR (5Gy). DNA (blue, Hoechst). Scale bar, 10 μm. **(C–D)** Bar-graphs indicating the average BRCA1 or 53BP1 foci number in $CycA^{+}$ cells. **(E)** Representative plots of traffic light reporter assay in U87shCTR and U87shC8 cells 72 h after induction. Homologous Recombination (HR) was assessed by reconstitution of GFP, while Non-Homologous End Joining (NHEJ) was visualized via mCherry. **(F)** Mean percentage GFP- (HR) and mCherry- (NHEJ) positive cells with standard deviation of three independent experiments. The correlation between independent experiments is visualized by estimation plots **(G). (H)** MTS assay measuring U87-MG cell viability inhibition after 72 h from IR. U87shCTR and shC8 cells were pre-treated 1 h before IR with the indicated inhibitors (RAD51i, 27 μM; DNAPKi, 2 μM) and then irradiated or not with 10Gy IR. Statistical analysis was performed by the unpaired Student's t-test (ns = not significant; $^{**}P \leq 0.01$; $^{***}P \leq 0.001$). Results represent the mean of three independent experiments ± SD. (For interpretation of the references to color in this figure legend, the reader is referred to the Web version of this article.)

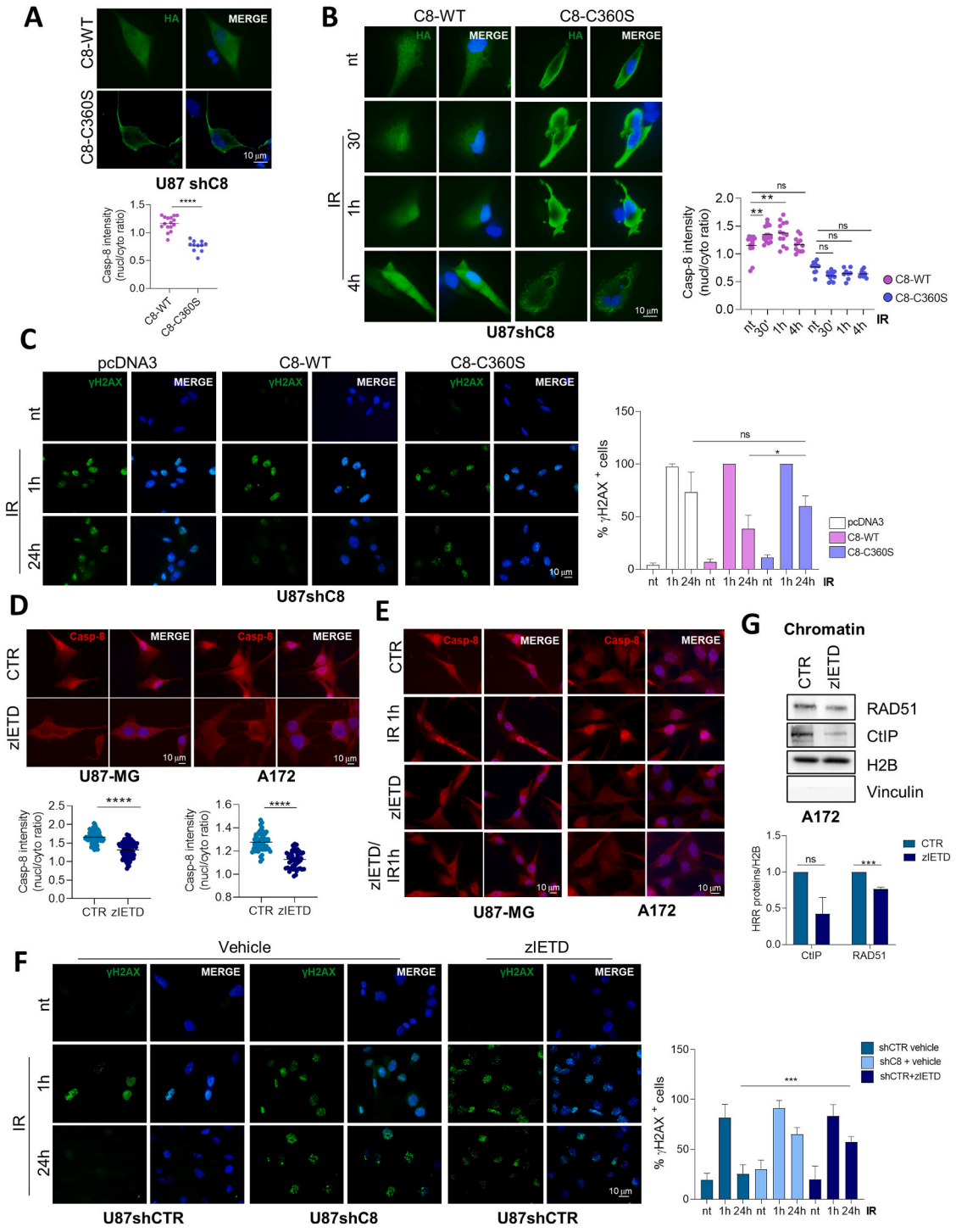

Fig. 5. Caspase-8 enzymatic activity is involved in Caspase nuclear localization and in DDR proficiency. (A–B) Immunofluorescence and relative analysis of U87shC8 and U87shC8 transiently transfected with the catalytic inactive Caspase-8 mutant (C8-C360S) showing Caspase-8 localization in basal condition (A) and upon IR (5Gy) (B). Caspase-8 (red), DNA (blue, Hoechst). Scale bar, 10 μm. **(C)** Immunofluorescence and relative quantification showing the percentage of cells (*i.e.,* U87shC8, U87shC8+C8-C360S) considered positive for the phosphorylation on Ser139 of the histone variant H2AX (n° γH2AX foci>5) at time 0 (not treated, nt) and 1 h–24 h post IR (5Gy); γH2AX (green), DNA (blue, Hoechst). Scale bar, 10 μm. **(D–E)** Immunofluorescence and relative analysis of U87-MG and A172 showing Caspase-8 localization treated or not with zIETD-FMK (50 μM) in basal condition (D) and post IR treatment (5Gy) (E). Caspase-8 (red), DNA (blue, Hoechst). Scale bar, 10 μm. **(F)** Immunofluorescence and relative quantification showing the percentage of U87shC8 cells and U87shCTR cells treated or not in the presence of zIETD-FMK (50 μM) considered positive for the phosphorylation on Ser139 of the histone variant H2AX (n° γH2AX foci>5) at time 0 (not treated, nt) and 1 h–24 h post IR (5Gy); γH2AX (green), DNA (blue, Hoechst). **(G)** Immunoblotting and relative densitometric analysis of chromatin insoluble portion derived from A172 treated or not with zIETD-FMK (50 μM) for 16hrs. H2B was used as chromatin loading control and Vinculin as cytoplasmic contamination control. Results represent the mean of three independent experiments ± SD. Statistical analysis was performed by the unpaired Student's t-test and Mann_Whitney test (ns = not significant; *P ≤ 0.05; **P ≤ 0.01; ***P ≤ 0.001; ****P ≤ 0.0001). (For interpretation of the references to color in this figure legend, the reader is referred to the Web version of this article.)

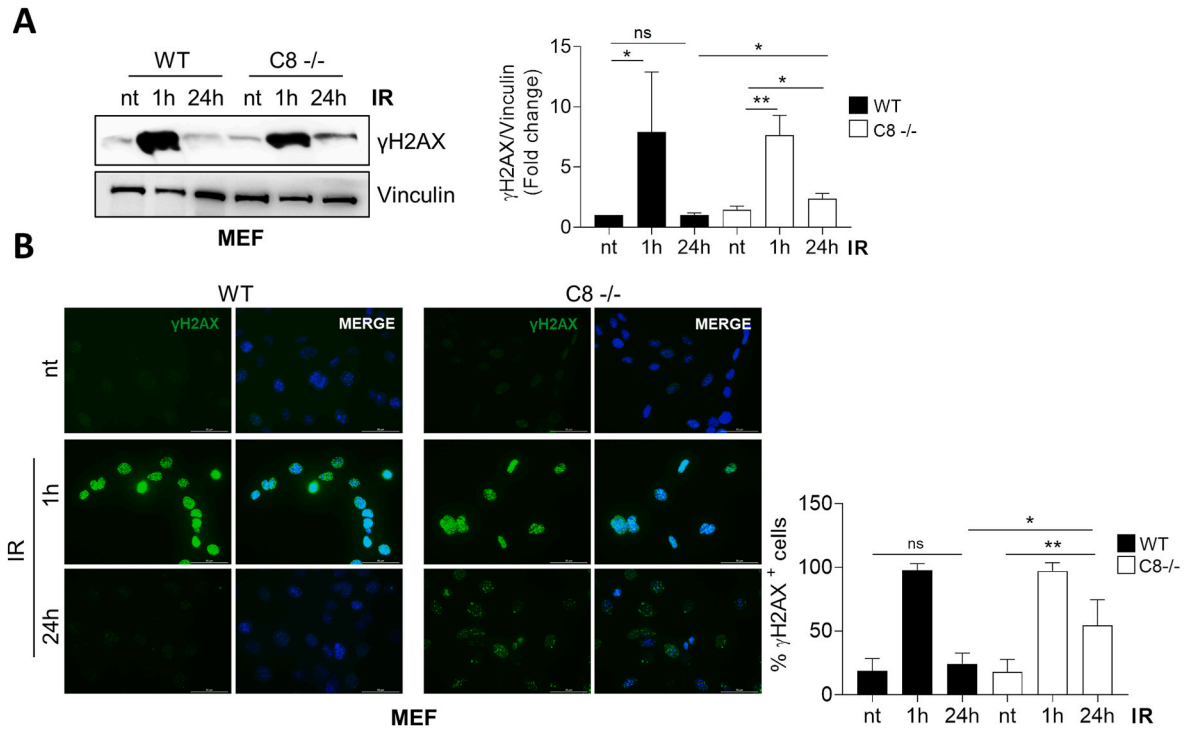

Fig. 6. Caspase-8 expression sustains DNA damage repair in murine embryo fibroblasts cellular model. (A) Immunoblotting and relative densitometric analysis showing γH2AX levels on total protein extracts from wild-type (*WT*) or Casp-8 knock-out (C8 −/−) MEFs. Vinculin was used as loading control. **(B)** Immunofluorescence and relative quantification showing the percentage of cells considered positive for the phosphorylation on Ser139 of the histone variant H2AX (n° γH2AX foci>5) at time 0 (not treated, nt) and 1 h–24 h post IR (5Gy); γH2AX (green), DNA (blue, Hoechst). Scale bar, 50 μm. Statistical analysis was performed by the unpaired Student's t-test (ns = not significant; *P ≤ 0.05; **P ≤ 0.01). Results represent the mean of three independent experiments ± SD. (For interpretation of the references to color in this figure legend, the reader is referred to the Web version of this article.)

2.7. Caspase-8 silencing in GBM cells confers sensitivity to PARP inhibition

We have previously demonstrated that GBM cells expressing Caspase-8 are more resistant to IR compared to the ones silenced for its expression [12].

Given both the role of Caspase-8 in HRR and the synthetic lethality between PARP inhibitors and HR defects [33], we speculated that lower Caspase-8 expression may sensitize irradiated cells to Olaparib, a competitive PARP-1/2 inhibitor [34]. To deepen this issue, we compared GBM shCTR and shC8 cell viability 72 h post the following treatments: DMSO (nt), Olaparib (Ola, 10 μM), IR (10Gy), and Olaparib combined with IR (Ola+IR). Silencing of Caspase-8 expression did not impair apoptosis (S6B) However, U87shC8 cells are more sensitive to the co-treatment, compared to shCTR cells, as revealed by MTS assay (Fig. 8A,B) and cytofluorometric analysis of cell death (Fig. 8C, D–Fig. S6B). Overall, these data prompt us to speculate a possible role of Caspase-8 as a novel DDR factor whose mutation or loss of expression may confer sensitivity to PARP inhibitors in combination with radiotherapy (Fig. 8E) [35].

3. Discussion

GBM is the most aggressive primary brain tumor in adults, characterized by substantial morbidity and mortality [4]. Its resistance to IR and TMZ is driven by hyperactive oxidative stress [36,37] and DNA repair responses [38,39]. Moreover, GBM is a very heterogeneous tumour comprising four gene expression-based subtypes: pro-neural, neural, classic and mesenchymal [40], the latter being the most aggressive and therapy-resistant [41,42]. In addition, treatment with IR and TMZ stimulates pro-neural to mesenchymal transition [43], selecting tumor cells with higher IR resistance, thus resulting in a poorer prognosis. Interestingly, the mesenchymal sub-type, typically characterized by PTEN and NF1 loss, is also characterized by high levels of Caspase-8 expression [40], which prompted investigations into how Caspase-8 might contribute to tumor survival and aggressiveness.

The discovery of non-canonical roles identified Caspase-8 as a central regulator of cell motility [10], tumorigenesis [11], inflammatory tumour microenvironment (TME) and neo-vascularization [12,13,44]. Interestingly, we have previously uncovered an inverse correlation between high Caspase-8 levels and the survival of GBM patients [13]. Moreover, we have demonstrated that GBM cells silenced for Caspase-8 expression display increased sensitivity to TMZ [13] and IR [12].

This study elucidates Caspase-8's critical role in therapy resistance in GBM by promoting DDR, particularly HRR. Notably, Boege et al. previously demonstrated Caspase-8's involvement in DDR through modulation of γH2AX foci formation in mouse hepatocytes [45]. Here, we demonstrate that Caspase-8 does not affect γH2AX foci formation but instead sustains the expression of key DDR factors involved in HRR, such as RAD51 and CtIP, and facilitates their recruitment to sites of DNA damage. We further found that Caspase-8 shuttles between the cytosol and nucleus, with transient nuclear accumulation following DNA damage, as previously reported in melanoma cells [9], and chromatin association. Here, we also unveil that Caspase-8 activity is required for Caspase-8 nuclear localization and DNA repair proficiency, supporting RAD51 and CtIP chromatin recruitment, but not their expression.

Interestingly, we provide evidence for a conserved role of Caspase-8 as promoter of DNA repair also in non - tumorigenic contexts *in vitro* and *in vivo*. Using the *Drosophila Melanogaster* model system, in which Caspase-8 plays apoptotic and non-apoptotic functions [28–30], we demonstrate that mutant larvae brains defective for Caspase-8 expression, display a significant accumulation of DNA damage upon IR compared to the *wt* counterpart, further supporting a key role of Caspase-8 as novel DNA repair player. Furthermore, using Caspase-8 $^{-/-}$

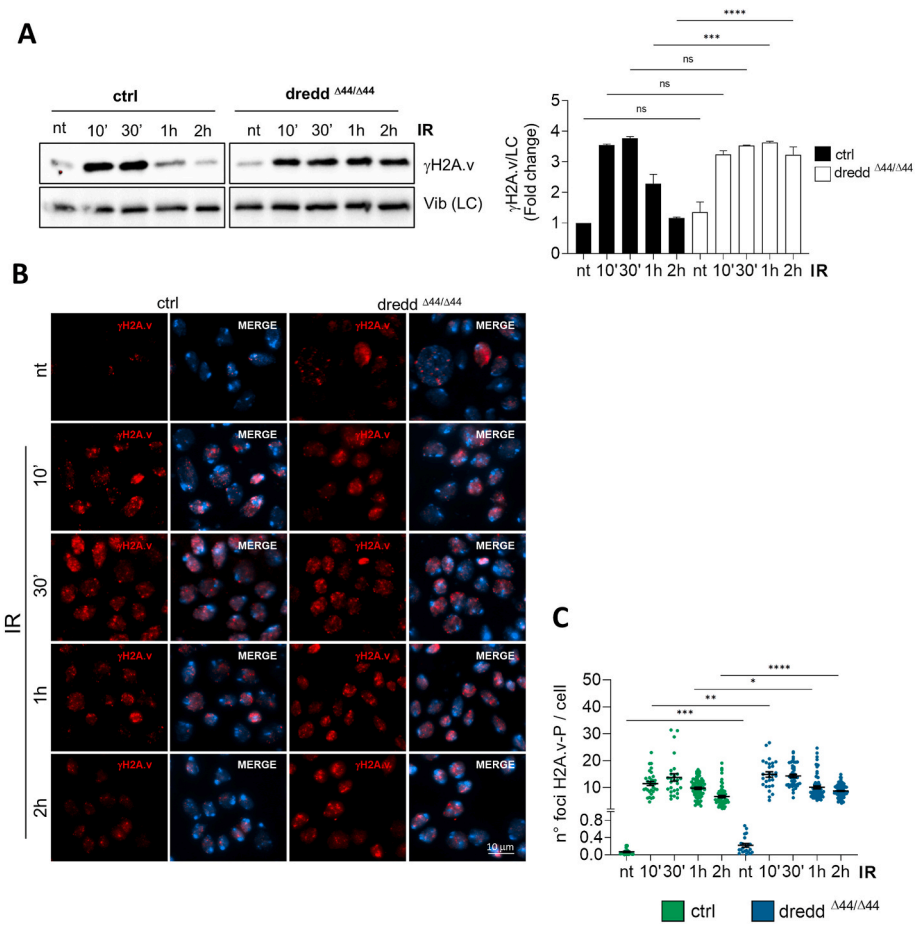

Fig. 7. Caspase-8 expression sustains DNA damage repair in *Drosophila melanogaster*. (A) Immunoblotting and relative densitometric analysis showing H2A.v phosphorylation (γH2A.v) levels on total protein extracts from *dredd*$^{\Delta 44}$ mutants (*dredd*$^{\Delta 44/\Delta 44}$) or wild-type (*WT*) *Drosophila* larval brains. Vibrator was used as loading control (LC). **(B–C)** Immunofluorescence and relative quantification showing the number of γH2A.v foci in nuclei from *dredd*$^{\Delta 4z4}$ mutants or *WT* larval brains at time 0 (not treated, nt), or 10′, 30′, 1 h and 2 h post IR, (5Gy); γH2A.v (red), DNA (DAPI, blue). Scale bar, 10 μm. Statistical analysis was performed by the non-parametric Kruskal-Wallis test (ns = not significant; *P ≤ 0.05; **P ≤ 0.01; ***P ≤ 0.001; ****P ≤ 0.0001). Each dot represents a specific field. Number of analyzed brains ≥3. (For interpretation of the references to color in this figure legend, the reader is referred to the Web version of this article.)

MEF, we provide evidence for this new role of Caspase-8 also in a non-tumoral context, where it has been previously demonstrated its involvement in the maintenance of chromosome stability [46]. In this context Caspase-8 together with RIPK1 has been suggested to modulate PLK1 activity therefore surveilling chromosome segregation and representing a safe-guardian of genomic instability [46].

Our data, highlight for the first time a direct role of Caspase-8 in the modulation of DNA repair, that may further support genome stability. Importantly, we can speculate that this function may have a dual role in cancer. Indeed, on one side Caspase-8 expression may counteract the accumulation of DNA damage and therefore protect cells from neoplastic transformation, but on the other side Caspase-8 by sustaining DNA repair may trigger cancer cell resistance to radio- and chemotherapy.

In this regard, the identification of Caspase-8 as a promoter of HRR pointed to Caspase-8 expression levels as a possible novel marker to select those tumors that may be more sensitive to the combined treatment with IR and PARP inhibitors (Fig. 8E). However, this issue was investigated only *in vitro* so far and therefore future studies, including orthotopic GBM models *in vivo,* are demanding to validate the translational relevance of Caspase-8 expression as a new biomarker for patient stratification.

4. Materials and methods

4.1. Cell culture

Glioblastoma cell lines (U87-MG, A172) and murine embryo fibroblasts (MEFs) were grown in Dulbecco Modified Eagle Medium (DMEM) (Sigma Aldrich), supplemented with 10 % south-american fetal bovine serum (Sigma Aldrich), 1 % L-Glutamine (Sigma Aldrich), streptomycin 10 mg/ml, penicillin 1000U/ml (Sigma Aldrich). Cells were cultured at 37 °C and 5 % CO_2. Glioblastoma patient-derived GBM39 cells were cultured as neurospheres in suspension in F-12 Medium supplemented with B27 Supplement (Gibco 17504044, 50x), EGF (20 ng/ml), and βFGF (10 ng/ml) as previously described [12]. All GBM cells were routinely tested negative for mycoplasma contamination.

4.2. Stable Caspase-8 knock-down in GBM cell lines

Stable interference of Caspase-8 was obtained through expression of two short-hairpin RNA (shRNA) as described in Ref. [12].

4.3. Stable or transient reconstitution of Caspase-8 wild-type

Stable and transient reconstitution of Caspase-8-WT in shC8 cell lines were performed as described in Ref. [12].

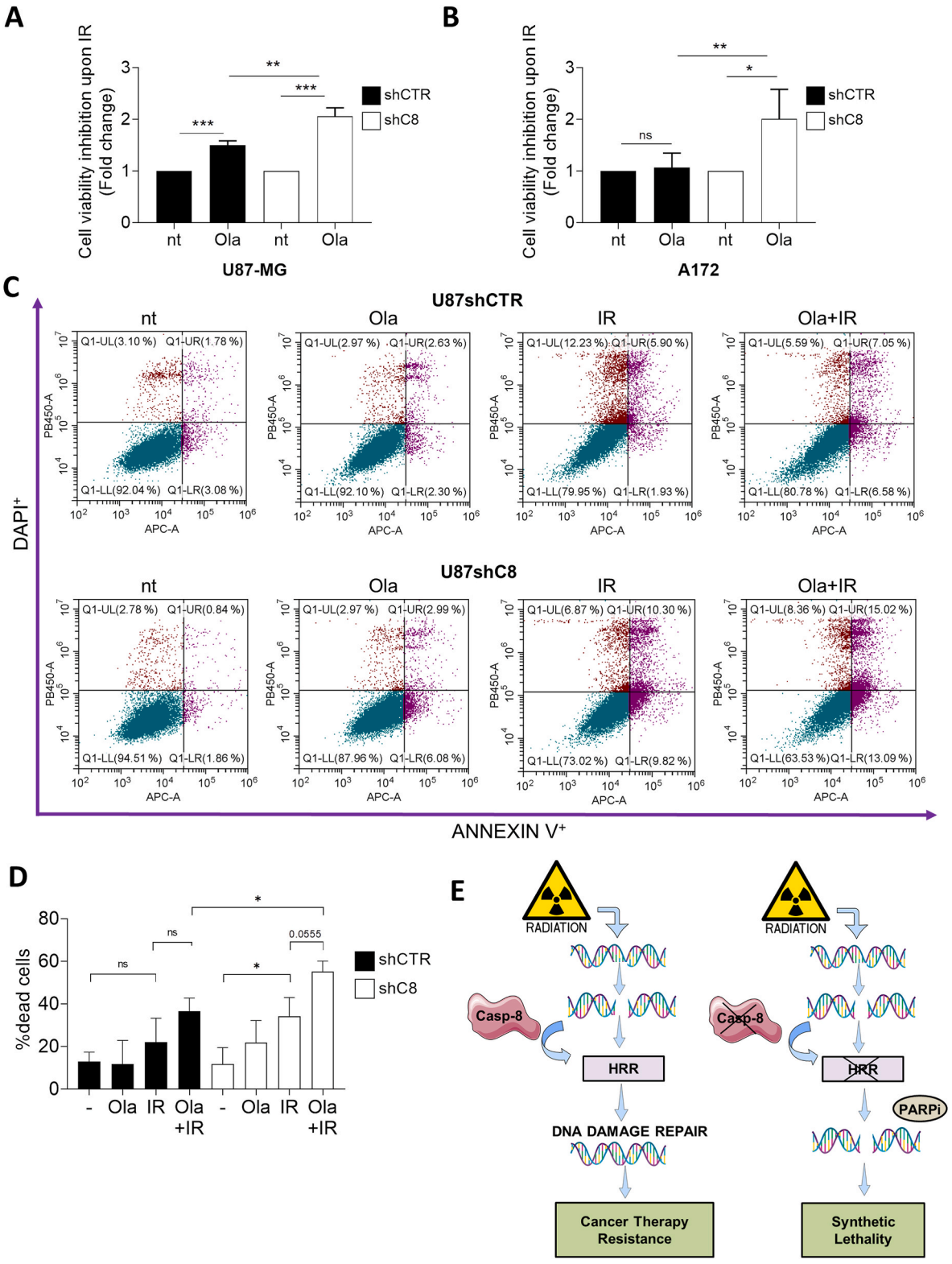

Fig. 8. Caspase-8 silencing promotes synthetic lethality in GBM cellular models. (A–B) MTS assay measuring cell viability in shCTR and shC8 cell (derived from U87-MG and A172) after 72 h from IR (10Gy). 1 h before irradiation shCTR and shC8 cells were pre-treated with Olaparib (10 μM). **(C–D)** Representative flow cytometry dot plot graphs and relative histogram of the percentage of dead cells upon AnnexinV-DAPI staining of U87shCTR and shC8 cells after 72 h irradiation (IR 10 Gy) pre-treated 2 h before IR with Olaparib (10 μM). Results represent the mean of three independent experiments ± SD. Statistical analysis was performed by One-way ANOVA statistical test for each cell lines compared to the untreated condition. Unpaired *t*-test was performed for shC8 Ola + IR condition compared to the respective shCTR condition. (ns = not significant; *p < 0.05; **p < 0.01; ***p < 0.001; ****p < 0.0001). **(E)** Schematic illustration of Caspase-8 function in DNA damage Repair in glioblastoma. Left panel: Caspase-8 expression in cancer supports Homologous Recombination Repair (HRR) and therapy resistance. Right panel: Loss of Caspase-8 expression results in defective HRR and enhances cancer cells sensitivity to combined treatments with IR and PARP inhibitors.

4.4. Antibodies and other reagents

Anti-BRCA1 (Santa Cruz Biotechnology, 1:250 sc-6954), anti-Caspase-8 (MBL 1:1000, 5F7), anti-CyclinA (Santa Cruz Biotechnology, 1:250, sc-596), anti-GAPDH (Santa Cruz 1:5000, D16H11), anti-pS139H2AX (Cell Signaling 1:300, 9781S), anti-53BP1 (Genetex 1:250, HL275), anti-Vinculin (Cell signaling 1:5000, 13901T), anti-ATM (Santa Cruz Biotechnology 1:500, 2C1), anti-pS1981-ATM (Cell Signaling 1:1000, 10H11.E12), anti-ATR (Bethyl 1:000, A300-137A), anti-pThr1989-ATR (Genetex 1:2000, GTX128145), anti-DNAPK (Cell Signaling 1:1000, 3H6), anti-pS2056-DNAPK (Sigma Aldrich 1:1000, SAB4504169), anti-CtIP (Genetex 1:500, 19E8), anti-RAD51 (Abcam 1:1000, AMab63801).

DNAPKi (NU7441, Sigma Aldrich) was dissolved in DMSO and given to cells at a concentration of 2 μM 1 h before DNA damage induction.

RAD51i (B02, Sigma Aldrich) was dissolved in DMSO and given to cells at a concentration of 27 μM l 1 h before DNA damage induction.

Neocarzinostatin (NCS, Sigma Aldrich) was dissolved in DMSO and given to cells at a concentration of 10 μM for 1hr.

zIETD-FMK (Selleck Chemicals) was dissolved in DMSO and given to cells at a concentration of 50 μM for 16hr.

Olaparib (Sigma Aldrich) was dissolved in DMSO and given to cells at a concentration of 10 μM 1 h before irradiation.

4.5. Protein extracts and immunoblotting

Cells were lysed in IP Buffer (50 mM Tris-HCL pH 7.5, 250 mM NaCl, 1 %NP40, 5 mM EDTA, 5 mM EGTA), or alternately in RIPA Buffer (50 mM Tris-HCL pH 8.0, 150 mM NaCl, 1 %NP40, 12 mM sodium deoxycholate), both supplemented with 1 mM phenyl-methyl-sulfonyl-fluoride, 25 mM NaF, 1 mM sodium orthovanadate, 25 mM β-glycerol-phosphate, 10 mg/ml TPCK, 10 mg/ml cocktail inhibitor. Protein extracts were separated and analyzed as described in Ref. [12].

4.6. Immunofluorescence

Cells were washed with 1x PBS and fixed in 4 % paraformaldehyde 10′ at room temperature. Cells were permeabilized with a 0.25 % PBS-triton solution for 5′ at room temperature. For γH2AX staining cells were additionally permeabilized in cold methanol for 10 min at −20 °C. After blocking for 1 h with 3 % BSA (Sigma Aldrich), primary antibodies were applied for 2 h at 37 °C or overnight at 4 °C. Secondary antibodies (Alexa Fluor 488, Cy5, Jackson ImmunoResearch) were used 1:300 for 45 min at 37 °C. Nuclei were stained with Hoechst 33342 for 10'. Images were acquired with a Zeiss confocal (LSM 800) or fluorescence microscope.

4.6.1. Neutral comet assay

DNA damage was assessed by Neutral Comet Assay as described in Ref. [47]. At least 300 comets per cell line were analyzed with Comet-Score v2.0 software.

4.7. MTS assay

U87-MG and A172 cell lines were pre-treated with inhibitors as indicated above and then treated with 10Gy IR. After radiation cells were plated 1000 per well in 96-well plates and grown for 48 h. Cellular viability was measured through Cell titer 96 AQueous One Solution Cell Proliferation Kit (Promega) using a VICTOR Multilabel plate reader.

4.8. Cytofluorimetric analysis

200,000 cells were plated in 60 mm dishes and treated after 24 h (DMSO, Olaparib 10 μM, IR 10 Gy, or both). Cell death was assessed 72 h post-IR using CytoFLEX S flow cytometry with Annexin V-APC and DAPI staining. Cell death was evaluated 72 h post-IR by using a CytoFLEX S (Beckman Coulter) instrument. Cells were collected, centrifuged for 5′ at 300g, and double-stained by using Annexin V-APC kit, according to the manufacturer's instructions (eBioscienceTM Annexin V Apoptosis Detection Kits; Thermo Fisher Scientific) and DAPI. Quality control was evaluated using CytoFLEX Daily QC Fluorospheres (Beckman Coulter). FCS files were analyzed using CytExpert version 2.2 software (Beckman Coulter). Dead cells (Annexin V+/DAPI + cells) were graphed as a percentage to control conditions.

4.9. Traffic light reporter

The traffic light (Sce target) reporter system was generated in U87-MG cells by lentivirus-mediated transduction and cells were selected using puromycin (2 μg/mL). Reporter cells were seeded subconfluently and induced for 72 h in triplicates with lentivirus vectors carrying partial GFP templates prior readouts. Analysis was performed using the Cytek Aurora flow cytometer and results visualized via FlowJo. Three independent experiments were performed and statistical significance was examined by paired *t*-test (Graphpad Prism).

4.10. In vivo experiments

4.10.1. Drosophila strains and rearing conditions

Drosophila stocks were maintained as described in Ref. [48]. All fly strains used come from the Bloomington Drosophila Stock Center (BDSC, Indiana University, Bloomington, IN, USA): w^{1118} (BDSC #3605) and $dredd^{\Delta 44}$ (BDSC #80924). The $dredd^{\Delta 44}/dredd^{\Delta 44}$ homozygous flies are viable and fertile.

4.10.2. Immunostaining and γ-H2Av foci detection

DNA damage in third instar larvae was induced with 5 Gy of X rays (Gilardoni MHF200 MD). Larval brains were fixed in 3,7 % formaldehyde at 10′, 30′1 h, 2 h post-IR. Brains were rinsed in PBS 0.1 % Triton (PBST), blocked 1 h at RT and incubated overnight at 4° with mouse anti-H2A.v-P 1:20 in PBS (DSHB AB_2618077), then washed in PBST and incubated for 2 h at RT with Rhodamine conjugated goat anti-mouse 1:50 (Jackson). Slides were mounted in Vectashield H-1200 with DAPI and analyzed on a fluorescence microscope (Zeiss Apotome; Zen Pro software). γH2A.v foci number was counted by using Fiji software (National Institute of Mental Health, Bethesda, Maryland, USA).

4.10.3. Immunoblotting

To determine the kinetics of H2Av phosphorylation, larvae were irradiated with X rays (5 Gy) and 20 brain samples were collected at different 0, 10′, 30', 1 h, 2 h post-IR. Brains protein extracts and immuoblotting were performed as in Ref. [49]. Primary antibodies were anti-H2Av-P mouse (1:500; DSHB AB_2618077) and anti-vibrator rabbit (1:5000; [48]).

4.11. Statistical methods

All data were analyzed and presented as mean of three independent experiments ± SD, except where differently specified. Significance was determined using Graph-Pad software, performing a two-tailed Student's t-test, or a two-way ANOVA. P-value <0.05 was considered significant (*), p-value <0.01 was considered very significant (**) and p-value <0.001 was considered extremely significant (***). The functional enrichment analysis was performed by querying EnrichR tool [50] and the p-values were adjusted for multiple comparison by using False Discovery Rate (FDR).

CRediT authorship contribution statement

Alessandra Ferri: Writing – review & editing, Writing – original draft, Validation, Supervision, Methodology, Investigation, Formal analysis, Data curation, Conceptualization. **Claudia Contadini:** Writing

– review & editing, Writing – original draft, Validation, Supervision, Methodology, Investigation, Formal analysis, Data curation, Conceptualization. **Claudia Di Girolamo:** Methodology, Investigation. **Claudia Cirotti:** Writing – review & editing. **Giulia Fiscon:** Software, Investigation. **Paola Paci:** Software, Investigation. **Marta Marzullo:** Methodology, Investigation. **Maria Pia Gentileschi:** Methodology. **Tatsuro Yamamoto:** Methodology. **Robert Strauss:** Methodology. **Donatella Del Bufalo:** Resources. **Laura Ciapponi:** Methodology, Investigation. **Daniela Barilà:** Writing – review & editing, Writing – original draft, Supervision, Resources, Funding acquisition.

Fundings

This work was supported by Associazione Italiana per la Ricerca sul Cancro (AIRC-IG2016-n.19069, AIRC-IG2021-n.26230, AIRC IG2020–n.24315, FIRC488); Italian Ministry of Health (RF-2016-02362022; GR-2021-12372614); American Italian Cancer Foundation Post-Doctoral Fellowship Award; Italian Ministery of Education and Research (DM 118/2023 to the PhD Program in Cellular and Molecular Biology, Department of Biology, University of Rome Tor Vergata; DM 1062/202).

Declaration of competing interest

The authors declare that they have no known competing financial interests or personal relationships that could have appeared to influence the work reported in this paper.

Acknowledgements

We are grateful to Venturina Stagni, Marco Barchi and Pietro Pichierri for data discussion and suggestions.

Glossary

53BP1, p53-binding protein 1; ATM, Ataxia-telangiectasia mutated; ATR, Ataxia Telangiectasia and Rad3-related; BRCA1, Breast Cancer gene 1; CtIP, C-terminal Binding Protein; DDR, DNA Damage Repair; DNA-PK, DNA-dependent protein kinase; DSBs, DNA double-strand breaks; FDR, False Discovery Rate; FCS, Flow Cytometry Standard; GBM, glioblastoma; Gy, gray; GFP, Green Fluorescent Protein; HR, Homologous Recombination; HRR, Homologous Recombination Repair; IR, Ionizing radiation; MEF, Murine Embryo Fibroblasts; NCS, Neocarzinostatin; NF1, Neurofibromatosis type 1; NF-κB, Nuclear Factor kappa-light-chain-enhancer of activated B cells; NHEJ, Non-Homologous End Joining; PTEN, Phosphatase and Tensin homolog; PLK1, Polo-like kinase 1; qRT-PCR, Quantitative Reverse Transcription PCR; RBBP8, RB Binding Protein 8, Endonuclease; RPK1, Receptor-interacting protein kinase 1; RNA-Seq, RNA sequencing; RT, Room Temperature; SD, standard deviation; TMZ, Temozolomide; TME, tumour microenvironment; WHO, World Health Organization; WT, wild type.

Appendix A. Supplementary data

Supplementary data to this article can be found online at https://doi.org/10.1016/j.canlet.2025.218120.

Data availability

All data in the manuscript are available in the Supplementary data, and raw data are available upon request.

References

[1] F.B. Furnari, T. Fenton, R.M. Bachoo, A. Mukasa, J.M. Stommel, A. Stegh, W. C. Hahn, K.L. Ligon, D.N. Louis, C. Brennan, et al., Malignant astrocytic glioma: genetics, biology, and paths to treatment, Genes Dev. 21 (2007) 2683–2710, https://doi.org/10.1101/gad.1596707.
[2] G.P. Dunn, M.L. Rinne, J. Wykosky, G. Genovese, S.N. Quayle, I.F. Dunn, P. K. Agarwalla, M.G. Chheda, B. Campos, A. Wang, et al., Emerging insights into the molecular and cellular basis of glioblastoma, Genes Dev. 26 (2012) 756–784, https://doi.org/10.1101/gad.187922.112.
[3] Q.T. Ostrom, H. Gittleman, L. Stetson, S.M. Virk, J.S. Barnholtz-Sloan, Epidemiology of gliomas, Cancer Treat Res. 163 (2015) 1–14, https://doi.org/10.1007/978-3-319-12048-5_1.
[4] R. Stupp, W.P. Mason, M.J. van den Bent, M. Weller, B. Fisher, M.J. Taphoorn, K. Belanger, A.A. Brandes, C. Marosi, U. Bogdahn, et al., Radiotherapy plus concomitant and adjuvant temozolomide for glioblastoma, N. Engl. J. Med. 352 (2005) 987–996, https://doi.org/10.1056/NEJMoa043330.
[5] S.S.K. Yalamarty, N. Filipczak, X. Li, M.A. Subhan, F. Parveen, J.A. Ataide, B. A. Rajmalani, V.P. Torchilin, Mechanisms of resistance and current treatment options for glioblastoma multiforme (GBM), Cancers (Basel) 15 (2023), https://doi.org/10.3390/cancers15072116.
[6] R. Scully, A. Panday, R. Elango, N.A. Willis, DNA double-strand break repair-pathway choice in somatic Mammalian cells, Nat. Rev. Mol. Cell Biol. 20 (2019) 698–714, https://doi.org/10.1038/s41580-019-0152-0.
[7] L. Krenning, J. van den Berg, R.H. Medema, Life or death after a break: what determines the choice? Mol Cell 76 (2019) 346–358, https://doi.org/10.1016/j.molcel.2019.08.023.
[8] D.G. Stupack, Caspase-8 as a therapeutic target in cancer, Cancer Lett. 332 (2013) 133–140, https://doi.org/10.1016/j.canlet.2010.07.022.
[9] I. Muller, E. Strozyk, S. Schindler, S. Beissert, H.Z. Oo, T. Sauter, P. Lucarelli, S. Raeth, A. Hausser, N. Al Nakouzi, et al., Cancer cells employ nuclear Caspase-8 to overcome the p53-Dependent G2/M checkpoint through cleavage of USP28, Mol Cell 77 (2020) 970–984 e977, https://doi.org/10.1016/j.molcel.2019.12.023.
[10] S. Barbero, A. Mielgo, V. Torres, T. Teitz, D.J. Shields, D. Mikolon, M. Bogyo, D. Barila, J.M. Lahti, D. Schlaepfer, et al., Caspase-8 association with the focal adhesion complex promotes tumor cell migration and metastasis, Cancer Res. 69 (2009) 3755–3763, https://doi.org/10.1158/0008-5472.CAN-08-3937.
[11] G. Fianco, C. Cenci, D. Barila, Caspase-8 expression and its Src-dependent phosphorylation on Tyr380 promote cancer cell neoplastic transformation and resistance to anoikis, Exp. Cell Res. 347 (2016) 114–122, https://doi.org/10.1016/j.yexcr.2016.07.013.
[12] C. Contadini, A. Ferri, M. Di Martile, C. Cirotti, D. Del Bufalo, F. De Nicola, M. Pallocca, M. Fanciulli, F. Sacco, G. Donninelli, et al., Caspase-8 as a novel mediator linking Src kinase signaling to enhanced glioblastoma malignancy, Cell Death Differ. 30 (2023) 417–428, https://doi.org/10.1038/s41418-022-01093-x.
[13] G. Fianco, M.P. Mongiardi, A. Levi, T. De Luca, M. Desideri, D. Trisciuoglio, D. Del Bufalo, I. Cina, A. Di Benedetto, M. Mottolese, et al., Caspase-8 contributes to angiogenesis and chemotherapy resistance in glioblastoma, eLife 6 (2017), https://doi.org/10.7554/eLife.22593.
[14] M. Kolesnichenko, C. Scheidereit, Synthetic lethality by PARP inhibitors: new mechanism uncovered based on unresolved transcription-replication conflicts, Signal Transduct Target Ther 9 (2024) 179, https://doi.org/10.1038/s41392-024-01893-2.
[15] H. Farmer, N. McCabe, C.J. Lord, A.N. Tutt, D.A. Johnson, T.B. Richardson, M. Santarosa, K.J. Dillon, I. Hickson, C. Knights, et al., Targeting the DNA repair defect in BRCA mutant cells as a therapeutic strategy, Nature 434 (2005) 917–921, https://doi.org/10.1038/nature03445.
[16] H.E. Bryant, N. Schultz, H.D. Thomas, K.M. Parker, D. Flower, E. Lopez, S. Kyle, M. Meuth, N.J. Curtin, T. Helleday, Specific killing of BRCA2-deficient tumours with inhibitors of poly(ADP-ribose) polymerase, Nature 434 (2005) 913–917, https://doi.org/10.1038/nature03443.
[17] C.E. Helt, W.A. Cliby, P.C. Keng, R.A. Bambara, M.A. O'Reilly, Ataxia telangiectasia mutated (ATM) and ATM and Rad3-related protein exhibit selective target specificities in response to different forms of DNA damage, J. Biol. Chem. 280 (2005) 1186–1192, https://doi.org/10.1074/jbc.M410873200.
[18] T. Stiff, M. O'Driscoll, N. Rief, K. Iwabuchi, M. Lobrich, P.A. Jeggo, ATM and DNA-PK function redundantly to phosphorylate H2AX after exposure to ionizing radiation, Cancer Res. 64 (2004) 2390–2396, https://doi.org/10.1158/0008-5472.can-03-3207.
[19] K.S. Prabhu, S. Kuttikrishnan, N. Ahmad, U. Habeeba, Z. Mariyam, M. Suleman, A. A. Bhat, S. Uddin, H2AX: a key player in DNA damage response and a promising target for cancer therapy, Biomed. Pharmacother. 175 (2024) 116663, https://doi.org/10.1016/j.biopha.2024.116663.
[20] A.N. Blackford, S.P. Jackson, ATM, ATR, and DNA-PK: the trinity at the heart of the DNA damage response, Mol Cell 66 (2017) 801–817, https://doi.org/10.1016/j.molcel.2017.05.015.
[21] C. Cirotti, C. Di Girolamo, I. Taddei, C. Contadini, G. Massacci, F. Sacco, D. Del Bufalo, I. Salvatori, C. Valle, D. Barila, Caspase-8 expression and its Src dependent phosphorylation on tyrosine 380 triggers NRF2 signaling activation in glioblastoma, Cell Death Differ. (2025), https://doi.org/10.1038/s41418-025-01542-3, 10.1038/s41418-025-01542-3.
[22] F. Zhao, W. Kim, J.A. Kloeber, Z. Lou, DNA end resection and its role in DNA replication and DSB repair choice in mammalian cells, Exp. Mol. Med. 52 (2020) 1705–1714, https://doi.org/10.1038/s12276-020-00519-1.

[23] B.S. Lopez, RAD51-mediated homologous recombination is a pro-tumour driver pathway, Oncogene 44 (2025) 4006–4016, https://doi.org/10.1038/s41388-025-03583-x.
[24] E. Orhan, C. Velazquez, I. Tabet, C. Sardet, C. Theillet, Regulation of RAD51 at the transcriptional and functional levels: what prospects for cancer therapy? Cancers (Basel) 13 (2021) https://doi.org/10.3390/cancers13122930.
[25] I. Cousineau, C. Abaji, A. Belmaaza, BRCA1 regulates RAD51 function in response to DNA damage and suppresses spontaneous sister chromatid replication slippage: implications for sister chromatid cohesion, genome stability, and carcinogenesis, Cancer Res. 65 (2005) 11384–11391, https://doi.org/10.1158/0008-5472.CAN-05-2156.
[26] T. Lei, S. Du, Z. Peng, L. Chen, Multifaceted regulation and functions of 53BP1 in NHEJ-mediated DSB repair (Review), Int. J. Mol. Med. 50 (2022), https://doi.org/10.3892/ijmm.2022.5145.
[27] M.T. Certo, B.Y. Ryu, J.E. Annis, M. Garibov, J. Jarjour, D.J. Rawlings, A. M. Scharenberg, Tracking genome engineering outcome at individual DNA breakpoints, Nat. Methods 8 (2011) 671–676, https://doi.org/10.1038/nmeth.1648.
[28] P. Chen, A. Rodriguez, R. Erskine, T. Thach, J.M. Abrams, Dredd, a novel effector of the apoptosis activators reaper, grim, and hid in Drosophila, Dev. Biol. 201 (1998) 202–216, https://doi.org/10.1006/dbio.1998.9000.
[29] C. Kietz, A. Meinander, Drosophila caspases as guardians of host-microbe interactions, Cell Death Differ. 30 (2023) 227–236, https://doi.org/10.1038/s41418-022-01038-4.
[30] F. Leulier, A. Rodriguez, R.S. Khush, J.M. Abrams, B. Lemaitre, The drosophila caspase dredd is required to resist gram-negative bacterial infection, EMBO Rep. 1 (2000) 353–358, https://doi.org/10.1093/embo-reports/kvd073.
[31] S. Baldi, P.B. Becker, The variant histone H2A.V of Drosophila–three roles, two guises, Chromosoma 122 (2013) 245–258, https://doi.org/10.1007/s00412-013-0409-x.
[32] C. Merigliano, A. Marzio, F. Renda, M.P. Somma, M. Gatti, F. Verni, A role for the twins protein phosphatase (PP2A-B55) in the maintenance of drosophila genome integrity, Genetics 205 (2017) 1151–1167, https://doi.org/10.1534/genetics.116.192781.
[33] N.Y.L. Ngoi, D. Gallo, C. Torrado, M. Nardo, D. Durocher, T.A. Yap, Synthetic lethal strategies for the development of cancer therapeutics, Nat. Rev. Clin. Oncol. 22 (2025) 46–64, https://doi.org/10.1038/s41571-024-00966-z.
[34] N. Dhanavath, P. Bisht, M.S. Jamadade, K. Murti, P. Wal, N. Kumar, Olaparib: a chemosensitizer for the treatment of glioblastoma, Mini Rev. Med. Chem. 25 (2025) 374–385, https://doi.org/10.2174/0113895575318854241014101928.
[35] C. Sun, A. Chu, R. Song, S. Liu, T. Chai, X. Wang, Z. Liu, PARP inhibitors combined with radiotherapy: are we ready? Front. Pharmacol. 14 (2023) 1234973 https://doi.org/10.3389/fphar.2023.1234973.
[36] C. Olivier, L. Oliver, L. Lalier, F.M. Vallette, Drug resistance in glioblastoma: the two faces of oxidative stress, Front. Mol. Biosci. 7 (2020) 620677, https://doi.org/10.3389/fmolb.2020.620677.
[37] R.P. Ostrowski, E.B. Pucko, Harnessing oxidative stress for anti-glioma therapy, Neurochem. Int. 154 (2022) 105281, https://doi.org/10.1016/j.neuint.2022.105281.
[38] S. Bao, Q. Wu, R.E. McLendon, Y. Hao, Q. Shi, A.B. Hjelmeland, M.W. Dewhirst, D. D. Bigner, J.N. Rich, Glioma stem cells promote radioresistance by preferential activation of the DNA damage response, Nature 444 (2006) 756–760, https://doi.org/10.1038/nature05236.
[39] A. Ferri, V. Stagni, D. Barila, Targeting the DNA damage response to overcome cancer drug resistance in glioblastoma, Int. J. Mol. Sci. 21 (2020), https://doi.org/10.3390/ijms21144910.
[40] R.G. Verhaak, K.A. Hoadley, E. Purdom, V. Wang, Y. Qi, M.D. Wilkerson, C. R. Miller, L. Ding, T. Golub, J.P. Mesirov, et al., Integrated genomic analysis identifies clinically relevant subtypes of glioblastoma characterized by abnormalities in PDGFRA, IDH1, EGFR, and NF1, Cancer Cell 17 (2010) 98–110, https://doi.org/10.1016/j.ccr.2009.12.020.
[41] J. Behnan, G. Finocchiaro, G. Hanna, The landscape of the mesenchymal signature in brain tumours, Brain 142 (2019) 847–866, https://doi.org/10.1093/brain/awz044.
[42] K.P.L. Bhat, V. Balasubramaniyan, B. Vaillant, R. Ezhilarasan, K. Hummelink, F. Hollingsworth, K. Wani, L. Heathcock, J.D. James, L.D. Goodman, et al., Mesenchymal differentiation mediated by NF-kappaB promotes radiation resistance in glioblastoma, Cancer Cell 24 (2013) 331–346, https://doi.org/10.1016/j.ccr.2013.08.001.
[43] J. Halliday, K. Helmy, S.S. Pattwell, K.L. Pitter, Q. LaPlant, T. Ozawa, E.C. Holland, In vivo radiation response of proneural glioma characterized by protective p53 transcriptional program and proneural-mesenchymal shift, Proc. Natl. Acad. Sci. U. S. A. 111 (2014) 5248–5253, https://doi.org/10.1073/pnas.1321014111.
[44] G. Fianco, C. Contadini, A. Ferri, C. Cirotti, V. Stagni, D. Barila, Caspase-8: a novel target to overcome resistance to chemotherapy in glioblastoma, Int. J. Mol. Sci. 19 (2018), https://doi.org/10.3390/ijms19123798.
[45] Y. Boege, M. Malehmir, M.E. Healy, K. Bettermann, A. Lorentzen, M. Vucur, A. K. Ahuja, F. Bohm, J.C. Mertens, Y. Shimizu, et al., A dual role of Caspase-8 in triggering and sensing proliferation-associated DNA damage, a key determinant of liver cancer development, Cancer Cell 32 (2017) 342–359 e310, https://doi.org/10.1016/j.ccell.2017.08.010.
[46] G. Liccardi, L. Ramos Garcia, T. Tenev, A. Annibaldi, A.J. Legrand, D. Robertson, R. Feltham, H. Anderton, M. Darding, N. Peltzer, et al., RIPK1 and Caspase-8 ensure chromosome stability independently of their role in cell death and inflammation, Mol Cell 73 (2019) 413–428 e417, https://doi.org/10.1016/j.molcel.2018.11.010.
[47] E. Malacaria, G.M. Pugliese, M. Honda, V. Marabitti, F.A. Aiello, M. Spies, A. Franchitto, P. Pichierri, Rad52 prevents excessive replication fork reversal and protects from nascent strand degradation, Nat. Commun. 10 (2019) 1412, https://doi.org/10.1038/s41467-019-09196-9.
[48] M. Marzullo, G. Romano, C. Pellacani, F. Riccardi, L. Ciapponi, F. Feiguin, Su(var) 3-9 mediates age-dependent increase in H3K9 methylation on TDP-43 promoter triggering neurodegeneration, Cell Death Discov. 9 (2023) 357, https://doi.org/10.1038/s41420-023-01643-3.
[49] S. Coni, F.A. Falconio, M. Marzullo, M. Munafo, B. Zuliani, F. Mosti, A. Fatica, Z. Ianniello, R. Bordone, A. Macone, et al., Translational control of polyamine metabolism by CNBP is required for drosophila locomotor function, eLife 10 (2021), https://doi.org/10.7554/eLife.69269.
[50] M.V. Kuleshov, M.R. Jones, A.D. Rouillard, N.F. Fernandez, Q. Duan, Z. Wang, S. Koplev, S.L. Jenkins, K.M. Jagodnik, A. Lachmann, et al., Enrichr: a comprehensive gene set enrichment analysis web server 2016 update, Nucleic Acids Res. 44 (2016) W90–W97, https://doi.org/10.1093/nar/gkw377.